Materials Transactions, Vol. 45, No. 7 (2004) pp. 2403 to 2409

Nondestructive Detection of Cold Flakes in Aluminum Alloy Die-Cast Plate with Ultrasonic Measurement

Hiroshi Kato[1], Tomoyuki Suzuki[1,*1], Yoshiharu Annou[1,*2] and Kensuke Kageyama[1]

Department of Mechanical Engineering, Faculty of Engineering, Saitama University, Saitama 338-8570, Japan

Aluminum alloy die-cast plates (ADC 12) were subjected to ultrasonic measurement to obtain a relation between the intensity distribution of the ultrasonic wave and positions of cold flakes appearing in the plate for developing a nondestructive method to detect cold flakes in the die-casts. Die-cast plates of 170 mm in length, 50 mm in width and 6.8 mm in thickness were produced with wider gates to introduce larger cold flakes in the plate. Then the ultrasonic measurement was carried out with the immersion method by using a probe generating a longitudinal wave of 20 MHz in frequency. Intensity distributions of the ultrasonic wave were obtained from the surface to the bottom. The cross section analysis was carried out to examine the distribution of the cold flake. From the cross section analysis, three types of cold flakes were observed: the type A with a straight boundary of initial solidification with oxide thin layer, the type B with a straight boundary without oxide layer, and the type C of an irregular and wavy boundary without oxide layer. In the case of the type C, the oxide layer was thought to be out of the observed section. The ultrasonic wave was slightly reflected from the front and rear boundaries between the cold flake and the matrix, and it was found that the position and the thickness of the cold flake can be detected by ultrasonic measurement.

(Received February 6, 2004; Accepted May 21, 2004)

Keywords: *nondestructive testing, ultrasonic testing, die-castings, aluminum alloy, casting defect, cold flakes, ultrasonic wave, backscattered wave*

1. Introduction

Aluminum die-casts have been widely used in many industries for their higher accuracy in shape and productivity. Die-cast products installed in machines, such as automobiles, often suffer repeated loading and thermal cycling in service, and cracks appear at casting defects to result in unexpected failure.

Casting defects are introduced in products during the casting process: molten metal is poured into a sleeve, and then injected in a permanent mold by a plunger. During pouring, the melt is rapidly cooled on an inner surface of a sleeve to result in formation of a thin solidified layer. When the melt is injected, the thin solid layer is scraped off, broken into small pieces and then pushed in the permanent mold.[1–3] These small pieces are called as cold flakes, cold fills or scattered structures (hereafter referred to as "cold flake"), and have a thin oxide layer contaminated by lubricant. Poor wetting of the oxide layer with the matrix causes crevice at a boundary between the cold flake and the matrix by relatively low forces, and hence the strength of die-cast products is largely reduced.[4–9] Therefore it has been very important to detect cold flakes in the die-cast products for assurance of quality. Although pores and cavities also reduce the strength of the die-casts.[10,11] they can be detected using the X-ray radiography because of large difference in transmissibility from the matrix. On the contrary, detection of cold flakes by the X-ray radiography is difficult because the cold flake and the matrix have the same transmissibility. So far, the cold flakes have been detected only by destructive methods, such as observation of cross sections of the products. This process is time-consuming, and also it is difficult to apply this process to all products.

When the ultrasonic wave propagates in metallic materials, the ultrasonic wave is scattered at grain boundaries and the wave intensity is decreased depending on the grain size.[12] Recently, the authors[13–16] developed a method to evaluate a thickness of a re-melted layer formed on a surface of aluminum alloy castings from the intensity distribution of the backscattered wave. Since the grain size in the re-melted layer was smaller than that of the matrix, the intensity of the backscattered wave in the former was smaller than that in the latter. Therefore a boundary between the re-melted layer and the matrix was evaluated from the intensity change of the backscattered wave. Cold flakes are formed in die-cast products by rapid cooling, and the grain size in the cold flake is smaller than that of the matrix. Therefore the intensity of the backscattered wave in the cold flake is expected to be smaller than that in the matrix. Also, the ultrasonic wave can be reflected from the oxide layer formed on the cold flake. From these aspects, the cold flake can be detected by the intensity distribution of the ultrasonic wave.

The present work is concerned with nondestructive detection of cold flakes appearing in the aluminum alloy die-casts through the ultrasonic measurement. Aluminum alloy die-cast plates containing larger cold flakes were fabricated, and then the ultrasonic measurement was conducted to obtain a relation between the intensity distribution of the ultrasonic and the microstructure in the die-casts.

2. Experimental Procedure

2.1 Preparation of specimen

Aluminum alloy plates of JIS-ADC 12 (Al-11Si-2Cu) were produced with a cold chamber die-cast machine. The plate was 170 mm in length, 50 mm in width and 6.8 mm in thickness, and shot in the longitudinal direction of the plate (hereafter referred to as the flow direction) with different shot time lags. Casting conditions and the chemical composition

*1Undergraduate Student, Saitama University. Present address: Kubota Corp., Naniwa 556-8601, Japan

*2Undergraduate Student, Saitama University. Present address: JATCO Ltd., Shimizu 417-8585, Japan

Table 1 Casting conditions of aluminum alloy die-casts.

Condition	
Method of die-casting	Low speed injection
Casting temperature	953 K (680°C)
Casting pressure	75 MPa
Die temperature	423∼433 K (150∼160°C)
Chilling time	10 s
Shot time lag (STL)	2, 4, 5 s

Table 2 Chemical composition of aluminum alloy die-casts.

(mass%)

	Al	Si	Cu	Mg	Zn	Fe	Mn	Ni	Sn
ADC 12	Res.	10.78	2.28	0.16	0.52	1.04	0.31	0.06	0.02

of the plate are tabulated in Tables 1 and 2. To obtain a relation between the intensity distribution of the ultrasonic wave and the distribution of the cold flake, larger cold flakes were introduced in the plate by using inlet and outlet gates of 1.7 mm × 30 mm and 1.4 mm × 20 mm, respectively.

Die-cast plates were subjected to the X-ray radiography under conditions of 110 kV in tube voltage and 5 mA in tube current for detection of casting defects. Then they were sectioned into three pieces of about 50 mm square, and top and bottom surfaces were polished with an emery paper of #1500 for ultrasonic measurement.

2.2 Ultrasonic measurement

The ultrasonic measurement was conducted with a measurement system as shown in Fig. 1 with the immersion method by using a focal-type wide-band probe (probe diameter of 12.7 mm) generating a longitudinal wave of 20 MHz in frequency with a focal distance of 25.4 mm in water. In the measurement, a water path was 11 mm so that the ultrasonic wave was focused at a half thickness position of the specimen. As shown in Fig. 2, the ultrasonic wave was measured at 800 points (40 points with 1 mm interval transversely to the flow direction and 20 points with 2 mm interval in the flow direction). For each specimen, data at 800 points were stored in a digital storage with a sampling time of

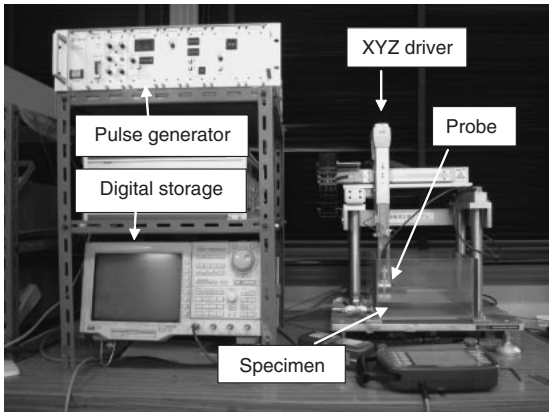

Fig. 1 Setup for ultrasonic measurement.

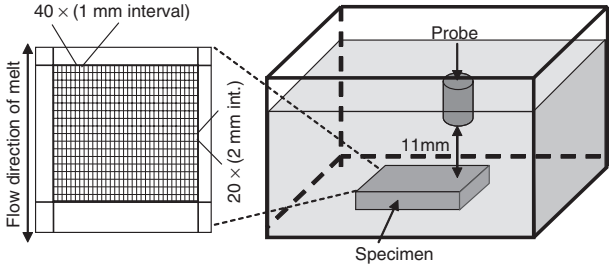

Fig. 2 Grid points and arrangement of specimen and probe for ultrasonic measurement.

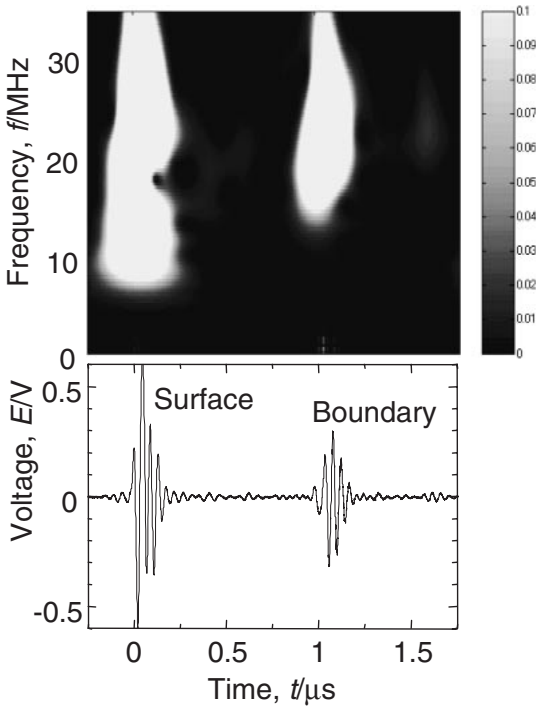

Fig. 3 Typical ultrasonic wave and mapping of wavelet analysis at a cross section containing cold flake.

0.5 ns and a sampling number of 10020, and then subjected to the Wavelet analysis with the Gabor function as the wavelet function to obtain an intensity distribution of the ultrasonic wave in a time-frequency domain. Figure 3 shows a typical ultrasonic wave and mapping of wavelet analysis. In the bottom figure, left and right echoes are those reflected from the specimen surface and a boundary between the cold flake and the matrix, respectively. A traveling time from the specimen surface to the cold flake was converted into a distance from the surface with the ultrasonic velocity of 6440 m/s determined by the preliminary measurement.

2.3 Observation of structure

After the ultrasonic measurement, specimens were sectioned transversely to the flow direction with 2 mm interval at positions of the ultrasonic measurement, and then polished. Cross sections were etched with a water solution of NaOH contained by 1 to 2 mass% to reveal the microstructure. Macroscopic views of the cross section were recorded by image scanner to examine positions of the cold flakes.

Microscopic observation of the cold flake was carried out through optical microscope.

3. Results and Discussion

3.1 Distributions of cold flakes in die-casts

Die-cast plates were subjected to the X-ray radiography. Figure 4 shows X-ray films (the left) and their sketches (the right). Rectangles marked in the films show positions of specimens used in the ultrasonic measurement. Numbers appearing on the top of the figures show the shot time lag in second. Large and small circles appeared in the figures are dints on the plate surface introduced in the casting process, and other marks are streaks or scratches on the plate surface. In the plates, no cold flake nor porosity was identified by the X-ray radiography.

The cross section analysis was carried out, and cold flakes were examined in many sections of the plates. As shown in Fig. 5, cold flakes of several mm in length appeared at a position marked on the photographs, and are far larger than that usually observed in the commercial die-casts. Although the plates were cast with different shot time lags, there was no difference of the distribution of the cold flake. From observation of the cold flakes, they were classified into three types such as,

Type A: Cold flakes containing a planar boundary between the cold flake and the matrix with a thin oxide layer

Type B: Cold flakes containing a planar boundary without the oxide layer

Type C: Cold flakes containing an irregular boundary without the oxide layer

Figure 6 shows an enlarged view of a typical planar boundary of the cold flake of the type A. Crystal grains in the cold flake are far smaller near the boundary than those in the matrix, and coarsened with increasing distance from the boundary. Although the planar surface was easily distinguished, it was difficult to distinguish a boundary between the cold flake and the matrix on the opposite side.

Nishi *et al.*[2] examined formation process of the irregular structures in aluminum alloy die-castings, and reported that there are three types of irregular structures: the scattered structure (the cold flake), the coarse α phase, and the massive structure, these irregular structures are formed under different solidification conditions in the shot sleeve. In the present experiment, types A and B are classified into the cold flake, and the type C can be classified into the massive structure because of no planar boundary. However it might contain the planar boundary out of the observed section.

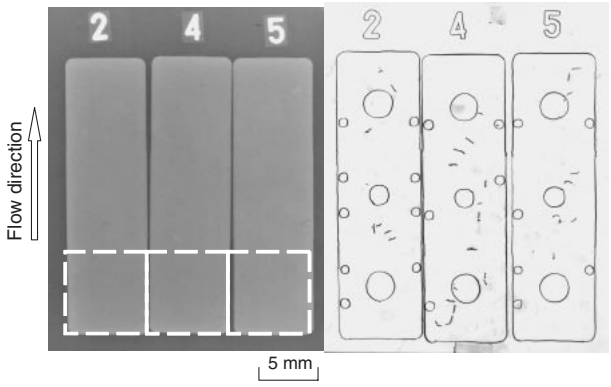

Fig. 4 X-ray films of die-cast plates and their sketches.

3.2 Relation between ultrasonic wave and cold flakes

The intensity change of the ultrasonic wave was examined at cross sections where the cold flake appears. The ultrasonic wave distribution for all types (A, B and C) are shown in Figs. 7 to 9. The ultrasonic measurement was carried out at a marked position in the top figure. In the bottom figure, a range of the cold flake (C.F.) is represented. Slight increase in

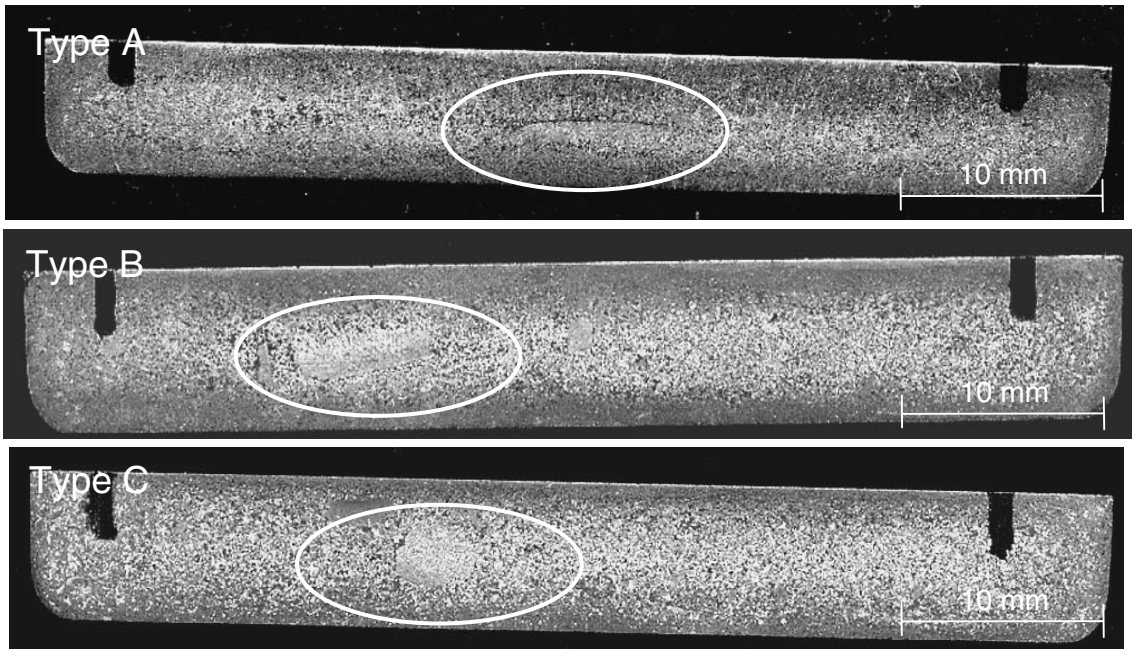

Fig. 5 Typical cold flakes observed on cross section of die-cast plate.

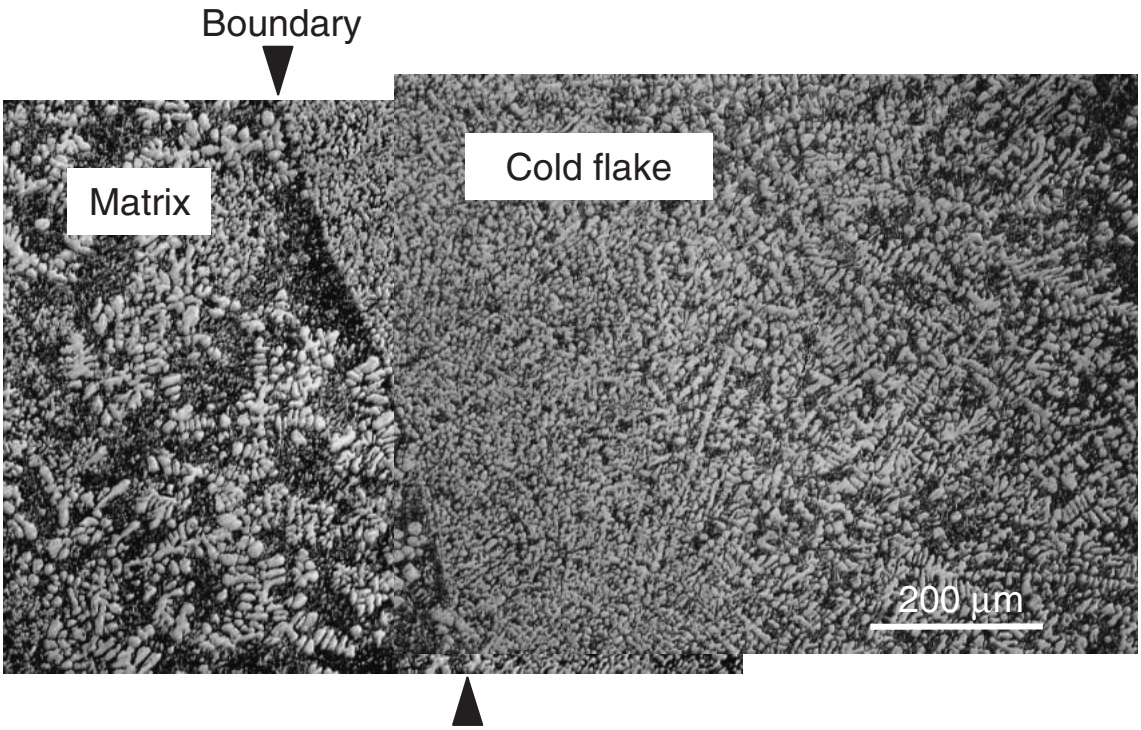

Fig. 6 Typical boundary between cold flake of type A and matrix.

the ultrasonic wave intensity was observed at the boundary between the cold flake and the matrix in all types.

There are two possibilities to increase the ultrasonic wave at the boundary: (1) difference in the structures of the matrix and the cold flake, and (2) existence of thin oxide layer at the boundary.

(1) ***Difference in structures***: The ultrasonic wave reflects from a boundary between regions of different acoustic impedances determined by the density and the sound velocity,[17] and these are influenced by the solute content and the grain size. When the molten alloy rapidly solidifies in the permanent mold, the solute content in the surface layer (a few mm in thickness) of the ingot is often greater than that inside the ingot due to inverse segregation.[18,19] Appearance of the inverse segregation is also expected in the cold flake because of rapid cooling of the melt on the surface of the sleeve. However, in the case of Al-Si alloys, sound velocities and the acoustic impedance can be different in the cold flake and the matrix only when the local solute segregation brings enrichment or dilution of Si particles in the cold flake. Moreover, Jiang *et al.*[16] showed that the acoustic impedance of the fine grained region in the aluminum alloy castings was not largely different from that of the coarse grained region and reflection from the boundary was very small. From these, in the case of the present work, the reflection due to different acoustic impedances by inverse segregation or different grain size may not occur at the boundary between the cold flake and the matrix.

(2) ***Existence of the oxide layer***: The initially solidified interface of the cold flake often contains thin oxide layer. The aluminum oxide has different density and elastic properties from the matrix (aluminum alloy), and hence the acoustic impedance of the oxide layer is largely different from that of

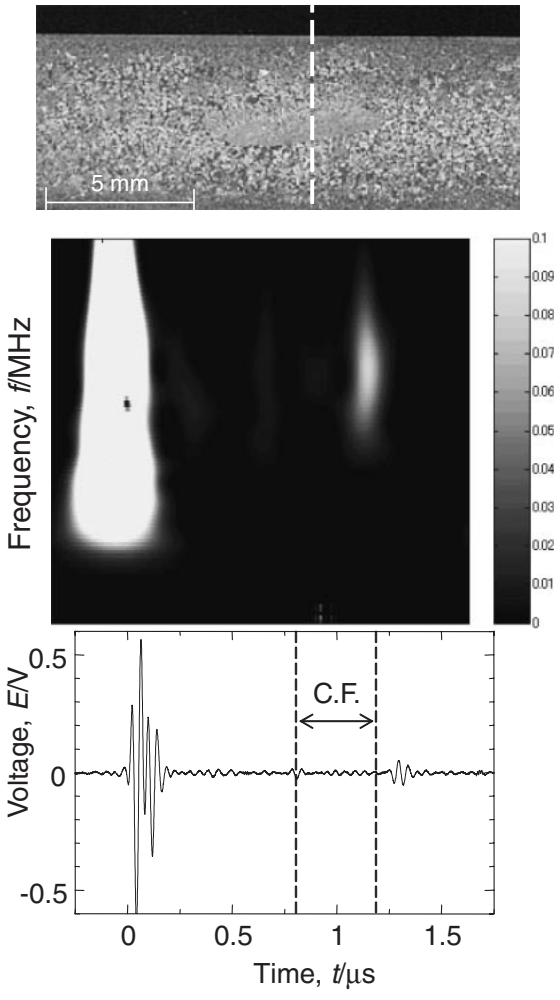

Fig. 7 Intensity distribution of ultrasonic wave at cold flake of type A.

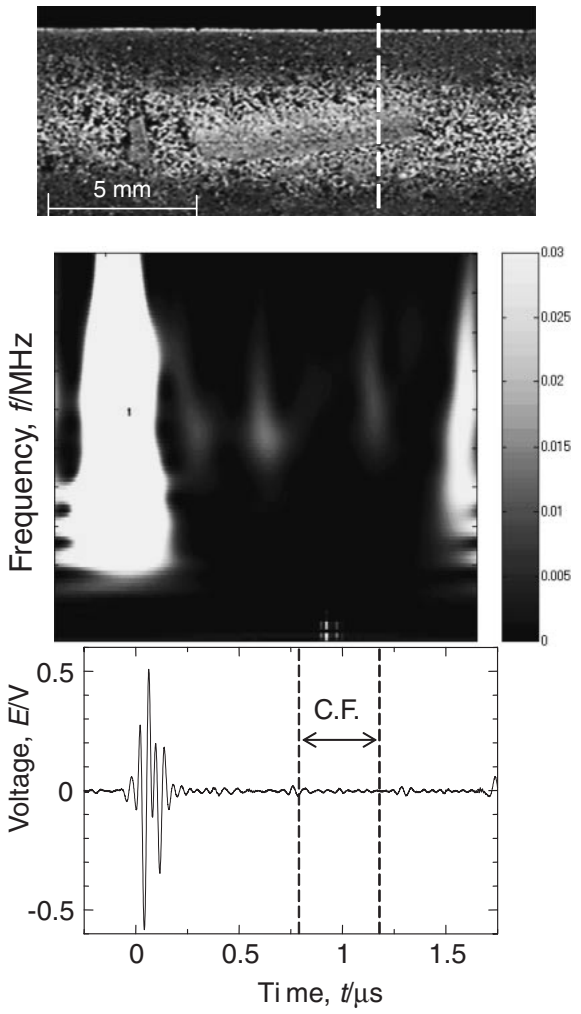

Fig. 8 Intensity distribution of ultrasonic wave at cold flake of type B.

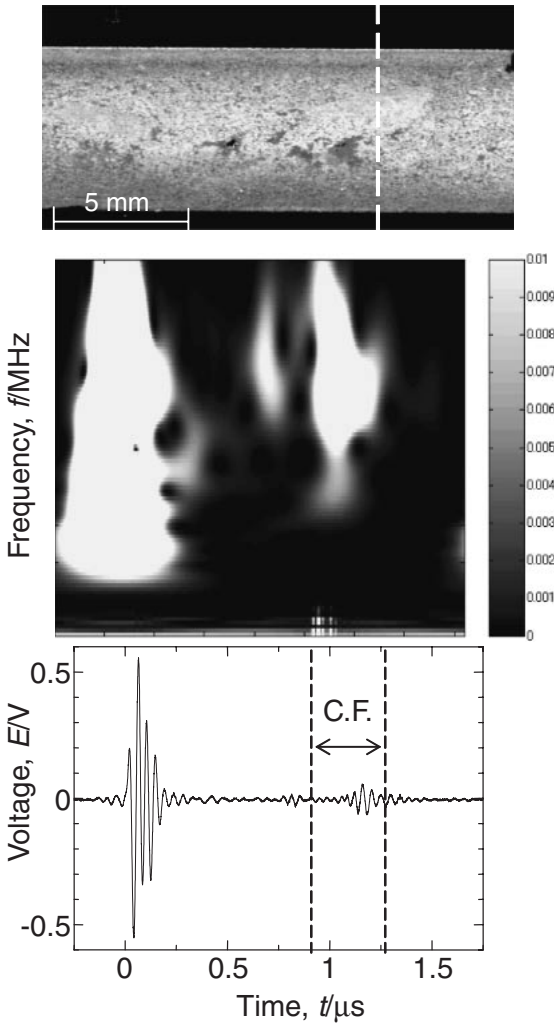

Fig. 9 Intensity distribution of ultrasonic wave at cold flake of type C.

the matrix to cause reflection of the ultrasonic wave from the oxide layer.[17] Also, the oxide layer usually exists with porosities, and the ultrasonic wave is reflected from porosities.[20] These caused reflection of the ultrasonic wave intensity from the boundary between the cold flake and the matrix.

From the above discussion, it was concluded that the ultrasonic wave intensity slightly increases at the boundary between the cold flake and the matrix due to reflection from the oxide layer at the initially solidified interface of the cold flake.

Since the grain size of the cold flake was smaller than that of the matrix, the attenuation of the ultrasonic wave was expected to be smaller in the cold flake than that in the matrix.[12] In the measurement of the intensity distribution of the ultrasonic wave in the present work, however, the wave intensity was not clearly decreased in the cold flake. In the present time, there is no reason why there was no change in the wave intensity in the cold flake.

Figure 10 compares a range of the cold flake of the type A estimated from the ultrasonic waveform and that measured on the cross section. A position of the boundary between the cold flake and the matrix was determined from the increase in the wave intensity in a cross section at which the cold flake

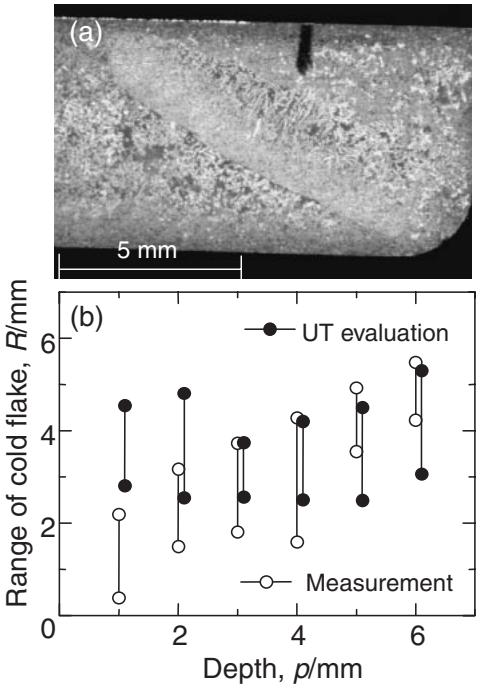

Fig. 10 Comparison of range of cold flake estimated from ultrasonic waveform and that measured on cross section.

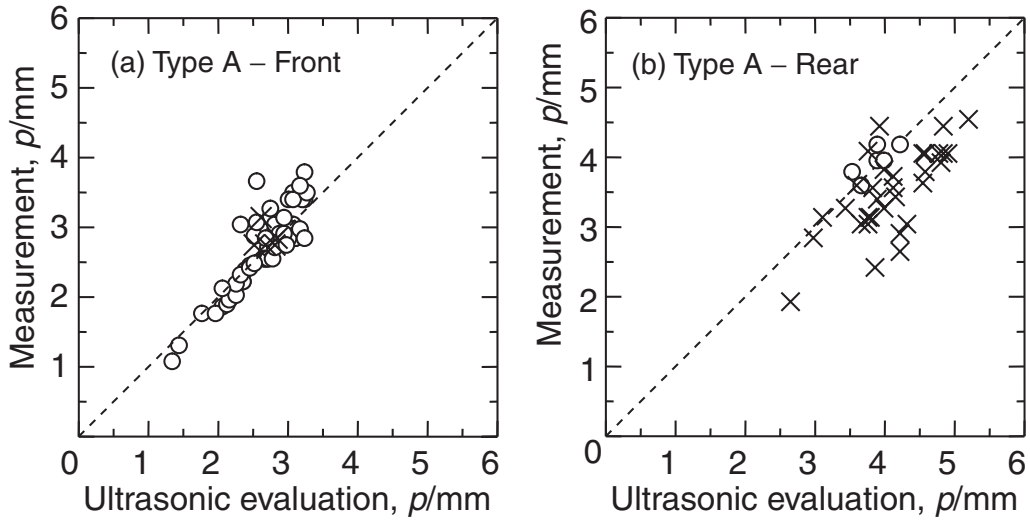

Fig. 11 Comparison of boundary position of cold flake of type A estimated from waveform analysis and those measured on cross section.

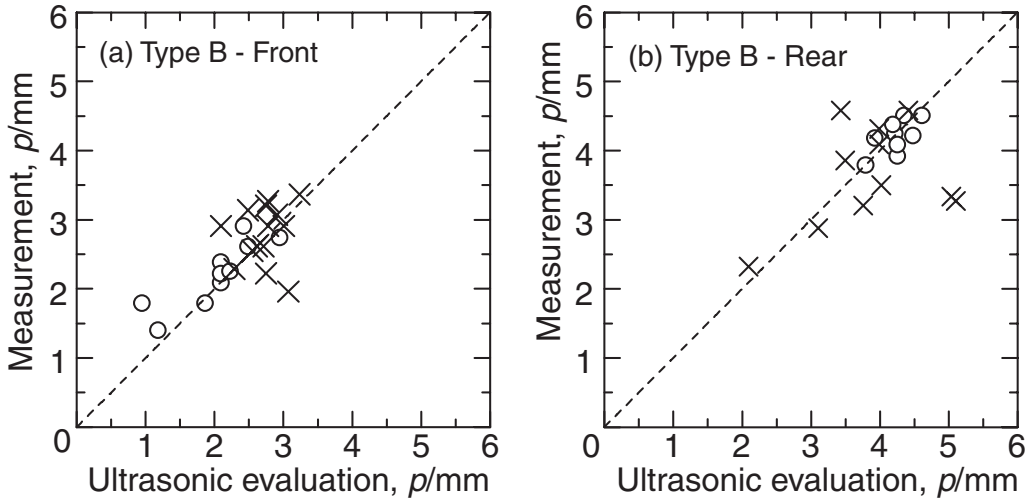

Fig. 12 Comparison of boundary position of cold flake of type B estimated from waveform analysis and those measured on cross section.

was observed. As shown in the figure, the estimated region of the cold flake is in good agreement with that measured at the cross section at a depth of 3 mm or more. When the cold flake was at a position 2 mm from the top surface or less, however, the estimated range was largely different from the measured one. This discrepancy was due to influence of trailing of the surface echo on the wave intensity distribution.

Figures 11 to 13 compare positions (the distance from the surface) of cold flakes of different types estimated from the ultrasonic wave intensity distribution and those measured on the cross section of the specimens. In the figures, open circles are positions of boundaries clearly observed on the cross section, and cross marks are those not clearly observed (the other side of the cold flake). In all cases, estimated positions are in good agreement with measured ones in the case of the clearly observed boundary. When the boundary was not clearly observed, coincidence was rather poor compared to the case of the clearly observed boundary. This was due to ambiguity in determining the boundary position.

From these results, it was found that the ultrasonic wave intensity increases at front and rear boundaries, and that the position and the thickness of the cold flake can be estimated from the ultrasonic measurement. By two dimensional scanning of the probe, as was done in the present work, the size of the cold flake can be estimated.

4. Conclusions

The aluminum alloy die-cast plates containing coarse cold flakes were produced, and then the ultrasonic measurement and the microstructure observation were conducted. Then following results are obtained.

(1) In the cross section, the cold flake was classified into three types, such as
Type A: straight boundary between the cold flake and the matrix with oxide layer
Type B: straight boundary without oxide layer
Type C: irregular and wavy boundary without oxide layer
In the case of the type C, it was thought that the oxide

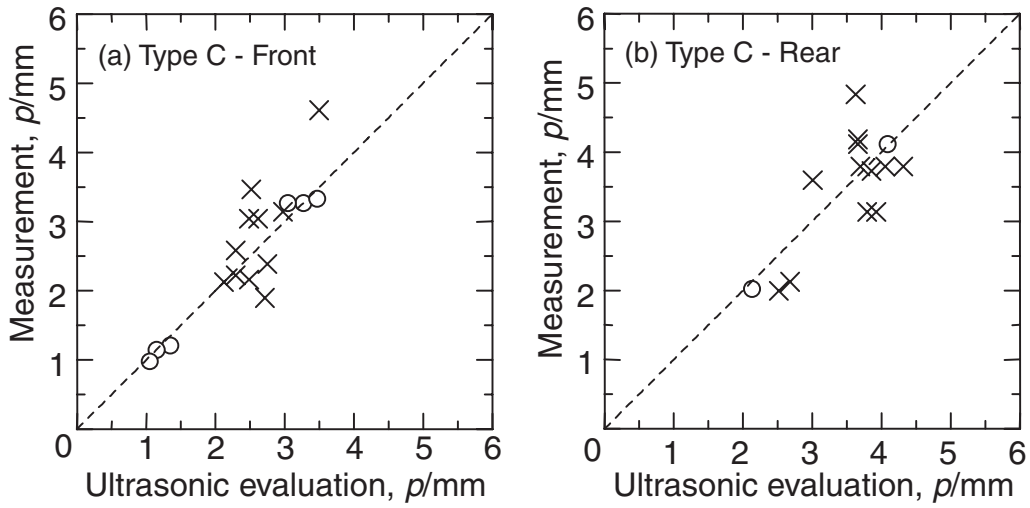

Fig. 13 Comparison of boundary position of cold flake of type C estimated from waveform analysis and those measured on cross section.

layer was out of the observed section.

(2) The ultrasonic wave intensity was increased at front and rear boundaries between the cold flake and the matrix.

(3) Although cold flakes in the die-casts were not detected by the X-ray radiography, the position and the thickness of the cold flake in die-cast products were detected or estimated by ultrasonic measurement.

Acknowledgements

The authors would like to thank Dr. N. Nishi, formerly with Ryobi Limited and presently with Japan Die Casting Association, and Mr. T. Komazaki with Ryobi Limited for their help to supply specimens. The X-ray radiography was carried out at the Technical Laboratory of Saitama Prefecture (presently, Saitama Industrial Technology Center).

REFERENCES

1) H. Iwahori, K. Tozawa, Y. Yamamoto and M. Nakamura: J. Japan Inst. Light Metals **34** (1984) 389–394. (in Japanese).
2) N. Nishi, T. Komazaki and Y. Takahashi: IMONO **63** (1991) 347–352. (in Japanese).
3) H. Nomura, E. Kato, Y. Maeda and S. Okubo: J. JFS **73** (2001) 656–661. (in Japanese).
4) W.G. Walkington: *Die Casting Defects*, (North American Die Casting Association, Rosemont, Illinois, 1997) pp. 155–158.
5) H. Iwahori, K. Tozawa, T. Asano, T. Yamamoto, M. Nakamura, M. Hashimoto and S. Uenishi: J. Japan Inst. Light Metals **34** (1984) 525–530. (in Japanese).
6) T. Komazaki, K. Matshuura and N. Nishi: IMONO **65** (1993) 191–196. (in Japanese).
7) T. Komazaki, Y. Maruyama and N. Nishi: IMONO **67** (1995) 258–264. (in Japanese).
8) M. Okayasu, K. Kanazawa and N. Nishi: J. JFS **70** (1998) 779–785. (in Japanese).
9) M. Avalle, G. Belingardi, M.P. Cavatorta and R. Doglione: Proc. Inst. Mech. Eng., Pt. L. J. Mater. Des. Appl. **216** (2002) 25–30.
10) M. Okayasu, K. Kanazawa and N. Nishi: J. JFS **71** (1999) 301–306. (in Japanese).
11) M. Avalle, G. Belingardi, M.P. Cavatorta and R. Doglione: Int. J. Fatigue **24** (2002) 1–9.
12) E.P. Papadakis: J. Acoust. Soc. Am. **37** (1965) 703–710.
13) G. Jiang, H. Kato, Y. Yoshida and T. Komai: *Nondestructive Characterization of Materials X*, Ed. R.E. Green, Jr., T. Kishi, T. Saito, N. Takeda and B. B. Djordjevic, (Elsevier, Oxford, UK, 2001) 185–191.
14) G. Jiang, H. Kato, Y. Yoshida and T. Komai: Insight **43** (2001) 743–747.
15) G. Jiang, H. Kato, Y. Yoshida and T. Komai: Materials Evaluation **59** (2001) 1421–1425.
16) G. Jiang, H. Kato, Y. Yoshida and T. Komai: NDT & E International **35** (2002) 221–225.
17) J. Krautkrämer and H. Krautkrämer: *Ultrasonic Testing of Materials*, 4th ed., (Springer-Verlag, Berlin, 1990) pp. 15–18.
18) W. V. Youdelis: *The Solidification of Metals*, (Iron Steel Inst., London, 1968) p. 112.
19) H. Kato and J. R. Cahoon: Metall. Trans. A **16A** (1985) 579–587.
20) J. Krautkrämer and H. Krautkrämer: *Ultrasonic Testing of Materials*, 4th ed., (Springer-Verlag, Berlin, 1990) pp. 93–102.